

Stress-modulated optical spin injection in bulk Si and GaAs semiconductors

J. L. Cabellos, Cuauhtémoc Salazar, and Bernardo S. Mendoza*

Division of Photonics, Centro de Investigaciones en Óptica, Loma del Bosque 115, León, Guanajuato, Mexico

(Received 3 June 2009; revised manuscript received 1 September 2009; published 7 December 2009)

A full band-structure *ab initio* calculation of the degree of spin polarization (DSP) in stressed bulk Si and bulk GaAs is reported. For Si, we found that compressive stress causes the DSP signal peak to decrease slightly in magnitude and to shift to higher energies. For expansive stress, the DSP signal shows a notable enhancement, changing from -31.5% for the unstressed case to $+50\%$ with only 1.5% of volumetric change. For GaAs, the only change induced due to either expansive or compressive stress is an energy shift of the DSP spectrum. This behavior may serve to tune the DSP in semiconductors to a suitable laser energy.

DOI: [10.1103/PhysRevB.80.245204](https://doi.org/10.1103/PhysRevB.80.245204)

PACS number(s): 72.25.Fe, 78.20.-e

I. INTRODUCTION

The study of spin injection into a nonmagnetic semiconductor is an important field of research in condensed-matter physics, known as spintronics, which has the potential of many applications.¹ The optical excitation of semiconductors with circularly polarized light creates spin-polarized electrons in the conduction bands.² The idea of using light for spin injection and detection dates back to 1968.³ Later it was shown that conversion of angular momentum of light into electron spin and vice versa is very efficient in III-IV semiconductors.² Known as “optical orientation,” this effect serves as an important tool in the field of spintronics, where it is used to spin polarize electrons. The injection of spin and the degree of spin polarization (DSP) in bulk GaAs, Si, and CdSe semiconductors has been reported recently,⁴ where a detailed comparison between a 30-band $\mathbf{k}\cdot\mathbf{p}$ model and a full band-structure LDA (local-density approximation)+scissors correction calculation was given. Some of the results obtained could be explained simply by using well-known features of the band structure and selection rules around the Γ points of GaAs and Si. However, for photon energies well above the band gap, the selection rules are more complicated, and full band-structure calculations are required to explore the DSP. For many semiconductors, such as CdSe, no $\mathbf{k}\cdot\mathbf{p}$ models are available, and the results of Nastos *et al.*⁴ indicate that the DSP can be reliably calculated with LDA+scissors corrected band structures. This suggests a program of study of optical orientation based on LDA+scissors calculations. Recently Salazar *et al.*⁵ have extended such theoretical study to several Si(111) surfaces, founding that these surfaces exhibit a DSP larger than the bulk Si DSP.

The purpose of this work is to calculate the DSP in stressed bulk Si and stressed bulk GaAs. We characterized applied stress by isometric volumetric strains, where the ratio of the volume at the stressed state to the volume at the unstressed state is employed as the independent input variable. We compute the DSP for a set of volumetric strains. To avoid structural changes, which are reported to arise at about 10% of volumetric change,⁶ we restricted our computations between the range of 1.5% of expansive strain and -1.5% of compressive strain.

The paper is organized as follows. In Sec. II we briefly present the basic expressions needed to evaluate the DSP. In Sec. III we show and discuss the results of the numerical evaluation of the DSP and accompanying functions for the

zinc-blende bulk semiconductors Si and GaAs, under compressive and expansive stress. Finally, in Sec. IV we present our conclusions.

II. THEORY

The theory of DSP is laid out by Nastos *et al.*,⁴ where we refer the reader for the details. Here, we only reproduce the most important expressions in order to calculate the DSP, which is formally defined along direction “a” as

$$\mathcal{D}^a = \frac{\dot{S}^a}{(\hbar/2)\dot{n}}, \quad (1)$$

where the rate of spin injection is given by $\dot{S}^a = \zeta^{abc}(\omega)E^b(-\omega)E^c(\omega)$ and the rate of carrier injection by $\dot{n} = \xi^{ab}(\omega)E^b(-\omega)E^c(\omega)$. Also,

$$\zeta^{abc}(\omega) = \frac{i\pi e^2}{\hbar^2} \int \frac{d^3k}{8\pi^3} \sum_{vcc'} \text{Im}[S_{c',c}^a(\mathbf{k})r_{vc'}^b(\mathbf{k})r_{cv}^c(\mathbf{k}) + S_{cc'}^a(\mathbf{k})r_{vc}^b(\mathbf{k})r_{c',v}^c(\mathbf{k})] \delta[\omega_{cv}(\mathbf{k}) - \omega], \quad (2)$$

is the (purely imaginary) pseudotensor that allows us to calculate the spin-injection rate, and

$$\xi^{ab}(\omega) = \frac{2\pi e^2}{\hbar^2} \int \frac{d^3k}{8\pi^3} \sum_{vc} \text{Re}[r_{vc}^a(\mathbf{k})r_{cv}^b(\mathbf{k})] \times \delta[\omega_{cv}(\mathbf{k}) - \omega], \quad (3)$$

is the tensor that allows us to calculate the carrier injection. The roman Cartesian superscripts are summed over if repeated. We remark that \mathcal{D}^a is a dimensionless quantity. Equation (2) takes into account the excited coherences of the conduction bands that are spin split by a small amount, typically smaller than the laser-pulse energy width with which one polarizes the electrons. Thus, this pulse excites a coherent superposition of two conduction bands. Even for very long pulses with narrow energy widths, dephasing effects lead to an energy width of the bands large enough that spin-split states can become quasidegenerate. Thus, these coherences were included by solving the equation of motion for the single-particle density matrix with the use of a multiple scale approach.⁴ Therefore, the prime in the sum of Eq. (2) is restricted to quasidegenerated conduction bands c and c' that

are closer than 30 meV, where this value is both a typical laser-pulse energy width and the room-temperature energy.⁴ As we show later, neglecting these coherences leads to wrong results. The matrix elements of the position operator $r_{nm}^a(\mathbf{k})$, the spin operator $S_{nm}^a(\mathbf{k})$, and the energy difference between valence (v) and conduction (c) states, $\omega_{cv}(\mathbf{k})$, are evaluated for \mathbf{k} points on a specially determined tetrahedral grid. This grid is used in the integrals of Eqs. (2) and (3) that are calculated through a linear analytic tetrahedral integration method.⁴ We assume, as is commonly done,² that the hole spins relax very quickly and we neglect them, focusing only on the electron spins; measurements have led to estimates of 110 fs for the heavy-hole spin lifetime in GaAs.⁷ We mention that the theoretical scheme neglects many-particle effects, electron-energy thermalization, electron-hole recombination, and phonon interaction, the latter limits the results to absorption across the direct band. The treatment of above effects is a theoretical challenge that ought to be pursued.

III. RESULTS

The calculations were performed in the framework of the density-functional theory within LDA+scissors correction, using the ABINIT plane-wave code.⁸ To include the spin-orbit interaction, we use the separable Hartwigsen-Goedecker-Hutter pseudopotentials⁹ within the LDA as parametrized by Goedecker *et al.*¹⁰ We exclude the semicore states (though they can be included with more computational effort), the contributions to the velocity matrix elements from the non-local part of the pseudopotential and from the spin-orbit interaction. However, we know that the contributions of the last two are small for Si.^{11–13} The scissors correction amounts to a rigid shift of \mathcal{D}^a along the energy axis by 0.87 eV for Si and 1.16 eV for GaAs, that are the values required to increase the LDA gap at the Γ point to their experimental value.^{14,15} Since the core electrons are neglected, we have eight electrons in the primitive unit cell with spin-up and spin-down wave functions, and thus eight valence bands. Consequently we found converged results with just eight conduction bands, along with a cutoff of 30 hartree and 18 424 \mathbf{k} points.

For Si and GaAs their corresponding crystal classes have the following nonzero components: $\zeta^{xy} = \zeta^{yx} = \zeta^{yz} = -\zeta^{zy} = -\zeta^{xz} = -\zeta^{zx}$ and $\xi^{xx} = \xi^{yy} = \xi^{zz} = \xi$. Using a circularly left-polarized electric field propagating along the $-z$ direction, i.e., $\mathbf{E} = E_0(\hat{x} - i\hat{y})/\sqrt{2}$ with E_0 its intensity, we get from Eq. (1) the DSP along the direction of propagation of the electric field as $\mathcal{D}^z = \zeta^{zy}/(\hbar\xi/2)$. Because of the relatively high symmetry of Si and GaAs, the exact crystal cut is unimportant; the injected spin density will always be aligned parallel or antiparallel to the laser beam. We characterized the applied stress by isometric volumetric strains. Then, we define $\sigma = a_s/a_0$ as the ratio of the lattice parameter of the stressed state, a_s , to the lattice parameter of the unstressed state, a_0 , where $a_0 = 5.39 \text{ \AA}$ (5.53 \AA), for the cubic unit cell of Si (GaAs). We use $a_s = \sigma a_0$ as the independent variable to calculate \mathcal{D}^z vs σ .

For Si we show in Fig. 1 the calculated \mathcal{D}^z vs the photon energy for several values of σ , including both expansive and

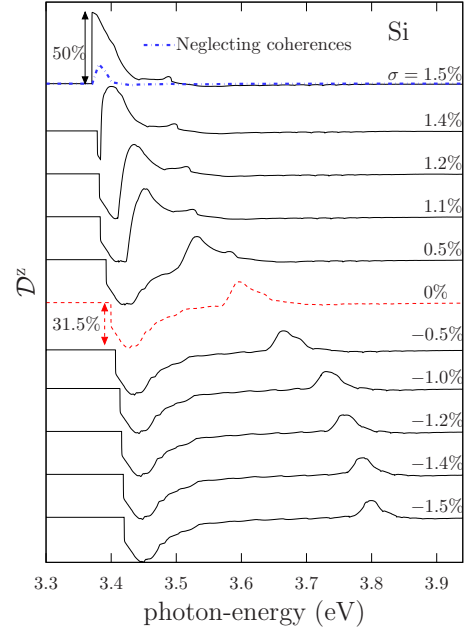


FIG. 1. (Color online) Stress modulation of the DSP, \mathcal{D}^z , vs photon energy for bulk silicon. Several spectra for different values of σ (expressed as percentage) are shown, where $\sigma > 0$ ($\sigma < 0$) is for expansive (compressive) stresses. The unstressed \mathcal{D}^z ($\sigma = 0\%$) is shown by a dotted line with a maximum value of $|\mathcal{D}^z| = 31.5\%$. For $\sigma = 1.5\%$, $\mathcal{D}^z|_{\max} = 50\%$. Neglecting the coherences in Eq. (2) leads to a wrong spectrum as shown for $\sigma = 1.5\%$. Each spectrum has been offset in the vertical axis for displaying purposes.

compressive strains, along with the unstressed ($\sigma = 0$) result. We vary σ from -1.5% to 1.5% . The unstressed spectrum shows two main features, one at 3.43 eV, just a few meV above the band gap with a -31.5% deep, and the other at 3.59 eV with a 15% peak. As we compress the unit cell ($\sigma < 0$) we see that the negative deep remains almost unchanged in magnitude and energy position, however the positive peak moves toward higher energies, keeping almost the same shape and showing a modest reduction to 11% at $\sigma = -1.5\%$. This situation changes radically when we expand the unit cell. Indeed, as σ increases the negative deep gets narrower, slightly moves to lower energies and then disappears at $\sigma = 1.403\%$. The positive peak in turn moves to lower energies, increases its height, and its shape changes until it gives a \mathcal{D}^z that rises sharply at the band edge with a maximum intensity of 50%. The spectrum at $\sigma = 1.5\%$ only shows this positive peak that has the largest $|\mathcal{D}^z|$ magnitude of all the spectra. Thus, under expansive stress bulk Si exhibits a quite interesting response: the negative deep and positive peak shown in \mathcal{D}^z for the unstressed unit cell coalesce into a single positive peak at the band edge with 75% of the spins polarized along the direction of propagation of the optical beam.¹⁶ We have checked that for $\sigma > 1.5\%$, the \mathcal{D}^z only shifts the spectrum to lower energies, retaining the magnitude of the DSP signal peak at 50%. Nevertheless such large expansions may be experimentally more difficult to achieve.¹⁷ Also, in Fig. 1 and only for $\sigma = 1.5\%$, we plot the \mathcal{D}^z without the coherences, that is equivalent to putting $c = c'$ in Eq. (2). We see that the coherences account for more

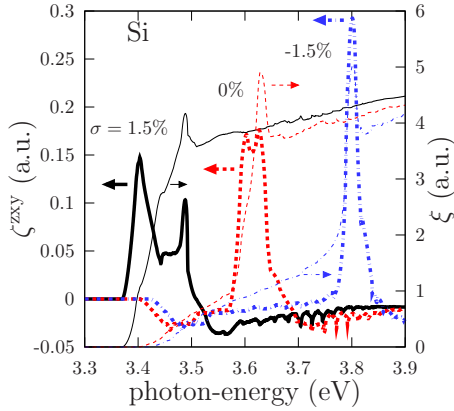


FIG. 2. (Color online) The calculated $\zeta^{zxy}(\omega)$ (thick lines) and $\xi(\omega)$ (thin lines) for Si vs photon energy for three different values of strain σ . The horizontal arrows point to the corresponding vertical scale of $\zeta^{zxy}(\omega)$ (left) and $\xi(\omega)$ (right).

than 70% of the total spectrum in this calculation, and neglecting them leads to unphysical results.

In Fig. 2 we show the calculated $\zeta^{zxy}(\omega)$ and $\xi(\omega)$ for $\sigma = 0, \pm 1.5\%$. We see that the onset at the band edge is redshifted in energy as σ goes from -1.5% to 1.5% . For both $\sigma = 0$ and -1.5% $\zeta^{zxy}(\omega)$ is negative around the onset, whereas it is positive for $\sigma = 1.5\%$ and rises very sharply. For $\xi(\omega)$ we see that the rise of the signal at the onset changes also with σ , being rather sharp for $\sigma = 1.5\%$ as it is for $\zeta^{zxy}(\omega)$. From these results, one can understand the line shape of D^z shown in Fig. 1. Indeed, the minimum (maximum) present in D^z for $\sigma = 0, -1.5\%$, comes from the minimum (maximum) in $\zeta^{zxy}(\omega)$, whereas the only one maximum of D^z for $\sigma = 1.5\%$ near the band edge comes from the maximum at $\zeta^{zxy}(\omega)$, but then the next local maximum in $\zeta^{zxy}(\omega)$ is barely seen in D^z since, as shown in the Fig. 2, the corresponding $\xi(\omega)$ is rather large as compared with $\zeta^{zxy}(\omega)$. In other words, the DSP depends strongly on the fine interplay between the ability for polarizing the spin of the electrons and the number of electrons (carriers) that one can inject.

In Fig. 3 we show for GaAs the calculated D^z vs the photon energy for three values of σ , one for expansive stress, one for compressive stress, and the other one for the un-

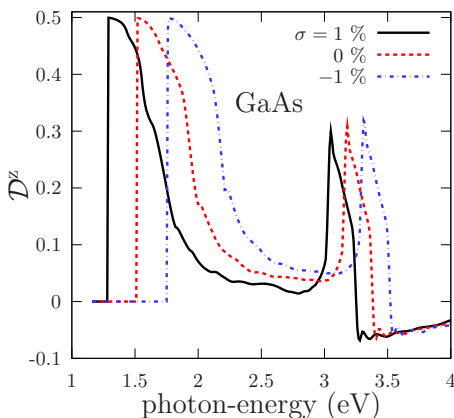


FIG. 3. (Color online) Stress modulation of the DSP, D^z , vs photon energy for bulk GaAs for three values of strain (σ).

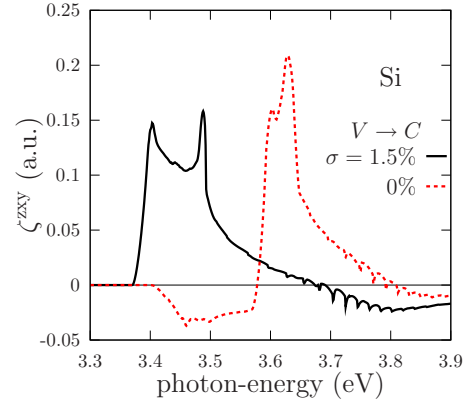


FIG. 4. (Color online) Analysis of the rate of spin injection, $\zeta^{zxy}(\omega)$, for the dominating transitions from the top valence band V to the bottom conduction band C at the band edge for $\sigma = 1.5\%$ and $\sigma = 0\%$.

stressed ($\sigma = 0$) result. The unstressed spectrum shows two positive peaks, one at 1.5 eV, just at the band edge of GaAs with $D^z = 50\%$, and the other at 3.18 eV with $D^z = 30\%$. As we expand (compress) the unit cell to $\sigma = 1\%$ ($\sigma = -1\%$) we see that the D^z spectrum shifts almost rigidly along the energy axis toward lower (higher) energies with only a very small change in the intensity of the peak at 3.1 eV. This behavior remains valid for larger values of $|\sigma|$. For the unstressed case of GaAs, the 50% value of the D^z has been confirmed experimentally,¹⁸ and explained theoretically,⁴ thus our calculated results indicate that either compressive or expansive strain will only move the onset of the signal. This also shows that the symmetry of the electronic band structure that leads into the results shown for $\sigma = 0$ remains basically the same as we apply the stress,⁴ in contrast with Si, where the changes in D^z are readily noticeable.

To gain an understanding of the rate of spin injection we proceed as follows. First we analyze the contribution of the different transitions toward $\zeta^{zxy}(\omega)$. In Fig. 4 we show $\zeta^{zxy}(\omega)$ for the transitions from the top valence band (V) to the bottom conduction band (C), for $\sigma = 0$ and $\sigma = 1.5\%$. These transitions have the most influential effect on the net spin-injection rate right at the band edge. The $V(C)$ band is doubly degenerated due to the spin degree of freedom. These transitions for $\sigma = 0$ have a $\zeta^{zxy}(\omega)$ that is first negative from 3.40 till 3.58 eV, and then becomes positive and goes to almost zero above 3.86 eV. However, for the same transitions at $\sigma = 1.5\%$, the corresponding $\zeta^{zxy}(\omega)$ is always positive and goes to almost zero above 3.9 eV. We note that for $\sigma = 0$ the signal kicks in 200 meV above the band gap, whereas for $\sigma = 1.5\%$ the signal kicks in just 32 meV above the band gap. This large difference in turn gives the D^z observed in Fig. 1, i.e., for $\sigma = 0$ we have a broad minimum at 25 meV above the band edge, followed by a broad maximum at 195 meV above the band edge, whereas for $\sigma = 1.5\%$ we have a sudden buildup of D^z at the band edge followed by a rapid decrease in the signal to zero.

To further understand the results we show in Fig. 5 the relevant energy bands for Si and GaAs for the corresponding \mathbf{k} values that determine the onset of D^z for three values of σ . We show the allowed transitions between the top valence

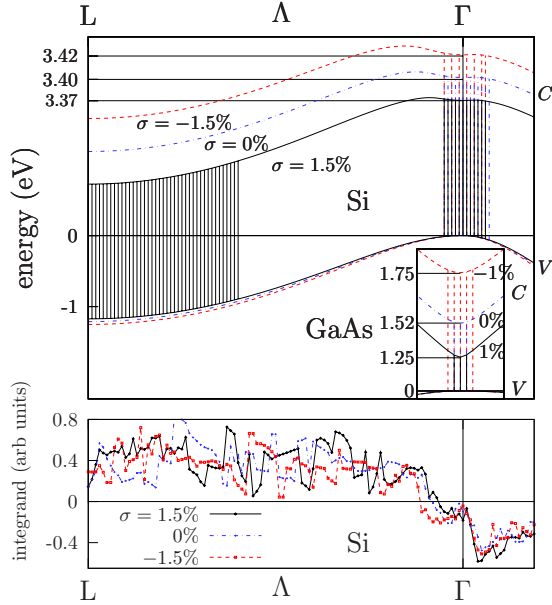


FIG. 5. (Color online) The top panel shows the relevant energy bands for Si and GaAs (inset) for the corresponding \mathbf{k} values that determine the onset \mathcal{D}^z for three values of σ . The valence bands are plotted with the same energy scale and the conduction bands are separated in energy for displaying purposes. The vertical lines are the allowed transitions between the top valence, V , and bottom conduction, C , bands for an energy range of 50 meV from the corresponding energy gap, E_g , of each σ . The vertical axis is not drawn to scale and the $E_g(\sigma)$ is shown for reference. The bottom panel shows the integrand of Eq. (2) for Si along the same Λ - \mathbf{k} path. Note that no other energy bands are shown, in particular, the spin-orbit split-off bands, although all the bands are included in the calculation.

band (V) and the bottom conduction band (C) for an energy range of 50 meV from the corresponding energy gap, E_g , of each σ . Thus, we cover the spectra of \mathcal{D}^z right at the onset (band edge) and 50 meV above it. The effect of expanding (compressing) the unit cells gives a value of E_g that is smaller (larger) than the corresponding value of E_g for the relaxed unit cell, and this in turn determines the onset of \mathcal{D}^z seen in the first four figures. We notice that for $\sigma = -1.5\%$ and 0% the allowed transitions for Si are only concentrated around the Γ point, whereas for $\sigma = 1.5\%$, besides having a similar region around Γ of allowed transition, there is also a rather wide region of allowed transitions along the Λ - \mathbf{k} path that extends all the way till the L point in the Brillouin zone. This is due to the fact that the top valence and bottom conduction bands are almost parallel (within 50 meV) for these values of \mathbf{k} , a behavior that is absent for $\sigma = 0, -1.5\%$. Thus the expansion of the unit cell changes the band structure in such a way that the bottom conduction band, along Λ , becomes (almost) parallel to the top valence band. For compression, the bottom conduction band does not change its curvature and remains the same as the corresponding band of the relaxed unit cell. The top valence band is almost insensitive to the change of the unit cell, at least for the region of the Brillouin zone shown, but of course this region is the only one relevant for the onset of the spin-polarized signal.

We mention that we do not show the other energy bands, such as the spin-orbit split-off band, for a clear presentation of the figure, however all the bands are properly taken into account in the calculation. In Fig. 5 we show the value of the \mathbf{k} integrand required in Eq. (2). We notice that for all three values of σ , the integrand is negative for values of \mathbf{k} around Γ , whereas for a large set of values of \mathbf{k} toward L along the Λ line, the integrand is positive. Thus, as the allowed transitions for $\sigma = -1.5\%$ and 0% are all concentrated around Γ the corresponding values of $\zeta^{xy}(\omega)$ are negative. In contrast with this, for $\sigma = 1.5\%$ the number of transitions coming from the Λ line, with a positive integrand, is much larger than those around the Γ point, with negative integrand, thus resulting in positive values for $\zeta^{xy}(\omega)$ and \mathcal{D}^z as shown in Figs. 1, 2, and 4, respectively. On the other hand, as we can see from Fig. 5 for GaAs, the allowed transitions are all concentrated around Γ , and the integrand (not shown) is only positive for the three values of σ . As a result we observe in Fig. 3, an almost rigid shift of \mathcal{D}^z as a function of σ , with no change in sign, in contrast to Si. A similar analysis could be carried out for any other energy, such as, for instance, the sudden change in sign seen at ~ 3.6 eV in Fig. 4, where transitions from other energy bands would be responsible for the signal.

IV. CONCLUSIONS

We have presented a study of optical spin-injection rates for stressed bulk Si and stressed bulk GaAs. Both compressive and expansive stress can effectively modulate the degree of spin polarization in these materials. For bulk Si, compressive stress shifts the positive peak of \mathcal{D}^z to higher energies and diminishes the signal about 20% of its value for the unstressed case. On the other hand, the negative deep remains almost unchanged both in energy position and magnitude. Contrary to this behavior, for expansive stress we found that the DSP signal is notably enhanced. For 1.5% of volumetric change the line shape of the signal changes from the one negative deep and one positive peak of the unstressed case to two positive peaks, one at the band edge with 50% of DSP and the other with an almost negligible magnitude. Thus, expansive strain changes the DSP from -31.5% of the unstressed case to 50%. Further expansion shifts this positive peak to lower energies without changing its magnitude. For bulk GaAs, compressive and expansive stress rigidly shift the spectrum to higher or lower energies, respectively, maintaining the band-edge peak signal at 50%. The results presented in this work show that the application of stress can be employed to tune the material to a suitable photon energy and, more importantly, to increase net DSP for the case of Si, making this material just as efficient as GaAs. We believe this ought to motivate the experimental verification of the theoretical results presented here.

ACKNOWLEDGMENTS

We acknowledge useful discussions with F. Nastos, J. Sipe and S. Turneaure. B.S.M. acknowledges partial support by CONACYT under Grant No. 48915-F, and C.S. and J.L.C. by CONACYT and CONCYTEG.

*bms@cio.mx

- ¹I. Zutic, J. Fabian, and S. D. Sarma, *Rev. Mod. Phys.* **76**, 323 (2004).
- ²M. I. Dyakonov and V. I. Perel, in *Optical Orientation*, edited by F. Meier and B. P. Zakharchenya (Elsevier, Amsterdam, 1984), Chap. 2, pp. 11–71.
- ³G. Lampel, *Phys. Rev. Lett.* **20**, 491 (1968).
- ⁴F. Nastos, J. Rioux, M. Strimas-Mackey, B. S. Mendoza, and J. E. Sipe, *Phys. Rev. B* **76**, 205113 (2007).
- ⁵C. Salazar, J. L. Cabellos, B. S. Mendoza, F. Nastos, T. Rangel, N. Arzate, and J. E. Sipe (unpublished).
- ⁶Stefan Turneaure, private communication.
- ⁷D. J. Hilton and C. L. Tang, *Phys. Rev. Lett.* **89**, 146601 (2002).
- ⁸X. Gonze, J.-M. Beuken, R. Caracas, F. Detraux, M. Fuchs, G.-M. Rignanese, L. Sindic, M. Verstraete, G. Zerah, F. Jollet, M. Torrent, A. Roy, M. Mikami, Ph. Ghosez, J.-Y. Raty, and D. C. Allan, *Comput. Mater. Sci.* **25**, 478 (2002).
- ⁹C. Hartwigsen, S. Goedecker, and J. Hutter, *Phys. Rev. B* **58**, 3641 (1998).
- ¹⁰S. Goedecker, M. Teter, and J. Hutter, *Phys. Rev. B* **54**, 1703 (1996).
- ¹¹B. S. Mendoza, F. Nastos, N. Arzate, and J. E. Sipe, *Phys. Rev. B* **74**, 075318 (2006).
- ¹²A. J. Read and R. J. Needs, *Phys. Rev. B* **44**, 13071 (1991).
- ¹³H. Kageshima and K. Shiraishi, *Phys. Rev. B* **56**, 14985 (1997).
- ¹⁴J. L. Cabellos, B. S. Mendoza, M. A. Escobar, F. Nastos, and J. E. Sipe, *Phys. Rev. B* **80**, 155205 (2009).
- ¹⁵F. Nastos, B. Olejnik, K. Schwarz, and J. E. Sipe, *Phys. Rev. B* **72**, 045223 (2005).
- ¹⁶Since in equilibrium there is an equal population of spin-up and spin-down electrons, the excess of optically injected spins, accounted for by \mathcal{D}^z , should be added to the existing population.
- ¹⁷Essentially, for a 0% to +8.5% volumetric expansion, the signal \mathcal{D}^z peak shifts from 3.5 to 1.5 eV, thus sweeping a large portion of the optical range.
- ¹⁸R. D. R. Bhat, P. Nemeč, Y. Kerachian, H. M. van Driel, J. E. Sipe, and A. L. Smirl, *Phys. Rev. B* **71**, 035209 (2005).